Journal of Magnetics 12(1), 40-44 (2007)

Planar Hall Sensor Used for Microbead Detection and Biochip Application

N. T. Thanh[1,2], D. Y. Kim[1], and C. G. Kim[1]*

[1]*Materials Science and Engineering and ReCAMM, Chungnam National University, Daejeon, Korea*
[2]*Nano Devices Research Center, Korea Institute of Science and Technology, Seuol, Korea*

(Received 14 March 2007)

The Planar Hall effect in a spin valve structure has been applied as a biosensor being capable of detecting Dynabeads® M-280. The sensor performance was tested under the application of a DC magnetic field where the output signals were obtained from a nanovoltmeter. The sensor with the pattern size of 50×100 μm^2 has produced high sensitivity; especially, the real-time profiles by using that sensor revealed significant performance at external applied magnetic field of around 7.0 Oe with the resolution of 0.04 beads per μm^2. Finally, a successful array including 24 patterns with the single sensor size of 3×3 μm^2 has shown the uniform and stable signals for single magnetic bead detection. The comparison of this sensor signal with the others has proved feasibility for biosensor application. This, connecting with the advantages of more stable and high signal to noise of PHR sensor's behaviors, can be used to detect the biomolecules and provide a vehicle for detection and study of other molecular interaction.

Keywords : planar hall sensor, biochip sensor, magnetic bead detection

1. Introduction

The discovery of giant magnetoresistive effect (GMR) in mid decade of 1980s has opened up a number of applications for magnetic sensors and devices. In the last few years, magnetoresistive sensors have also been proposed as potential detection components in biological devices such as highly sensitive biosensors and biochips based on a magnetic labeling platform [1-3]. Recently the detection of paramagnetic beads for biosensor application has been reported by use of Hall [4, 5] and Planar Hall sensor [6]; in which the Planar Hall sensor has been of more interest due to a nano-Tesla sensitivity and the reduction of temperature drift by at least four orders of magnitude, thus considerably improving upon the resolution and signal-to-noise of magnetoresistive sensors [7-9]. L. Ejsing *et al.* in their works have investigated the capability of magnetic microbead detection using Planar Hall effect in IrMn/NiFe bilayers. In an application for magnetic microbead detection, it is important to ensure a sufficient uniaxial anisotropy, a well-defined single domain state and the advantage of higher signal-to-noise than those of GMR or spin valve sensors with the single bead signal of 0.3 μV [10].

In our experiments, we proposed to utilize the Planar Hall Effect (PHE) in a spin valve structure for the single magnetic bead of Dynabeads® M-280 detection. The sensor structure incorporates free and pinned layers in which it was based on the resistance variation when the magnetization orientation in free magnetic layer rotates under the change of external applied magnetic field. The PHE sensor performances were reported to be a high signal and sensitive for Dynabeads® M-280 Streptavidin.

2. Experiment Procedure

The spin valve structure of Ta(5.0 nm)/NiFe(4.5 nm)/CoFe(1.5 nm)/Cu(2.6 nm)/CoFe(4.0 nm)/IrMn(10.0 nm)/Ta(5.0 nm) for patterned sizes of 100×50 μm^2 and Ta(5.0 nm)/NiFe(6.0 nm) /Cu(3.5 nm)/NiFe (3.0 nm)/IrMn(10.0 nm)/Ta(5.0 nm) for sensor array were fabricated by DC magnetron sputtering system under working pressure of 1.0 mTorr and the base pressure of 7.0×10^{-9} Torr on silicon dioxide wafer at room temperature. During sputtering process, a uniform magnetic field of 100 Oe was applied parallel to plane of films, which was used to induce a magnetic anisotropy of ferromagnetic layers and to align the pinning direction of the antiferromagnetic IrMn layer.

PHE sensors were prepared by lithography method into

*Corresponding author: Tel: +82-42-821-6632,
Fax: +82-42-822-6272, e-mail: cgkim@cnu.ac.kr

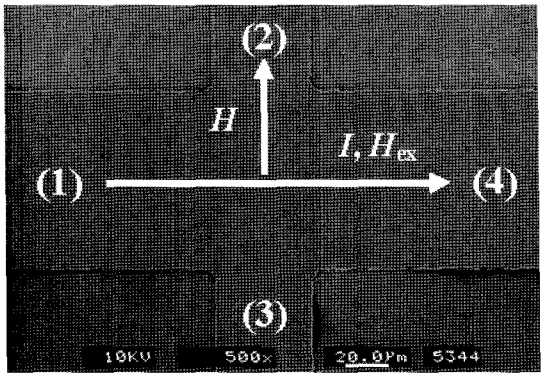

Fig. 1. SEM image of the electrodes for AMR and PHE measurements.

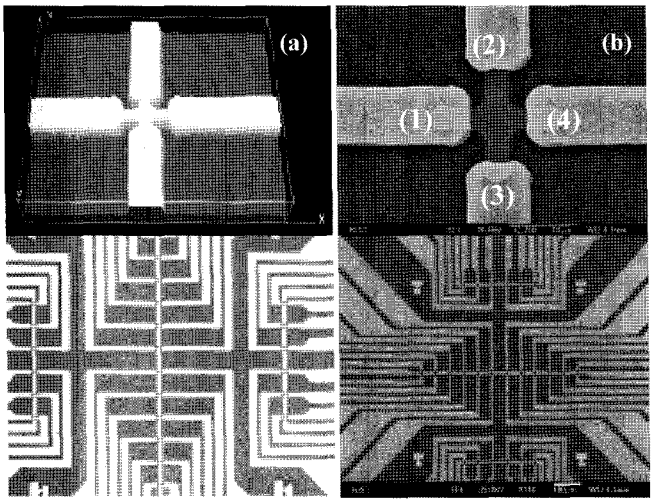

Fig. 2. Single sensor and BARC photos for magnetic bead detection, captued by photomicroscope (a) and SEM (b). The single sensor size of 33 μm^2 and Bead Array Counter (BARC) containing 24 sensors. All patterns were passivated by SiO_2 layer.

four electrode bars each pattern [11]. The sensors were passivated with a 150 nm thick sputtered SiO_2 layer to protect against the fluid used during experimentation. The easy axis of ferromagnetic (FM) layer and the direction of current were aligned along terminal 1 and terminal 4 with sensing current of 1.0 mA, as shown in Fig. 1 for 100×50 μm^2 sensor sizes; and in Fig. 2 for the array. The droplets of Dynabeads® M-280 solution were dropped on the surface of sensor and washed by pipet-lite SL-10. The sensor signals were obtained from terminal 2 and 3 under a magnetic field of various magnetic fields with nanovolt meter.

3. Results and Discussions

For the pattern size of 100×50 μm^2, the single sensor

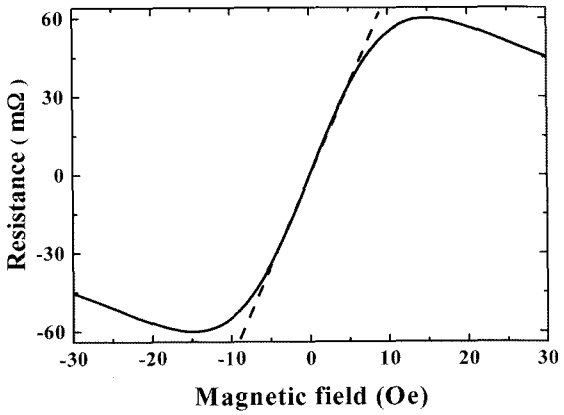

Fig. 3. The sensor transfer curve using Planar Hall resistance in spin-valve structure of Ta (5.0 nm)/ NiFe (4.5 nm)/CoFe (1.5 nm)/Cu (2.6 nm)/ CoFe (3.0 nm)/IrMn (10.0 nm)/Ta (5.0 nm), under various applied magnetic field at a fixed current of 1 mA.

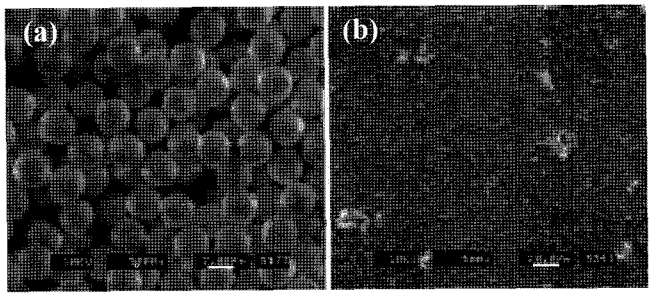

Fig. 4. The density of prototypal (a) and diluted (b) magnetic bead solution on the surface of sensor, observed by SEM photos.

transfer curve is shown in Fig. 3 where the PHR voltage is plotted versus an external applied magnetic field. The curve fitted well and a good agreement was obtained by using single domain model with an absence of hysteresis. From the performance, a high linear sensitivity profile was observed around 4.0 μV/(Oe.mA) [10]. It is larger than that compared with L. Ejsing's work around 2.0 μV/(Oe.mA) in structure of NiFe/IrMn/NiFe [11]. This, therefore, demonstrates that Planar Hall sensor used here is more sensitive to magnetic fields in the magnetic bead detection application.

Fig. 4(a) and (b) show the density of prototypal and 10% diluted magnetic beads on the surface of the sensor observed by SEM, respectively. The experiments for prototypal magnetic bead detection were carried out at applied magnetic fields from 0.0-10.0 Oe as shown in Fig. 5.

As shown in Fig. 6, for signal comparison, the output signals were 0.0 μV at an external applied magnetic field magnitude of 0.0 Oe and then increased as the magnetic field increases to 7.0 Oe; however the output signals de-

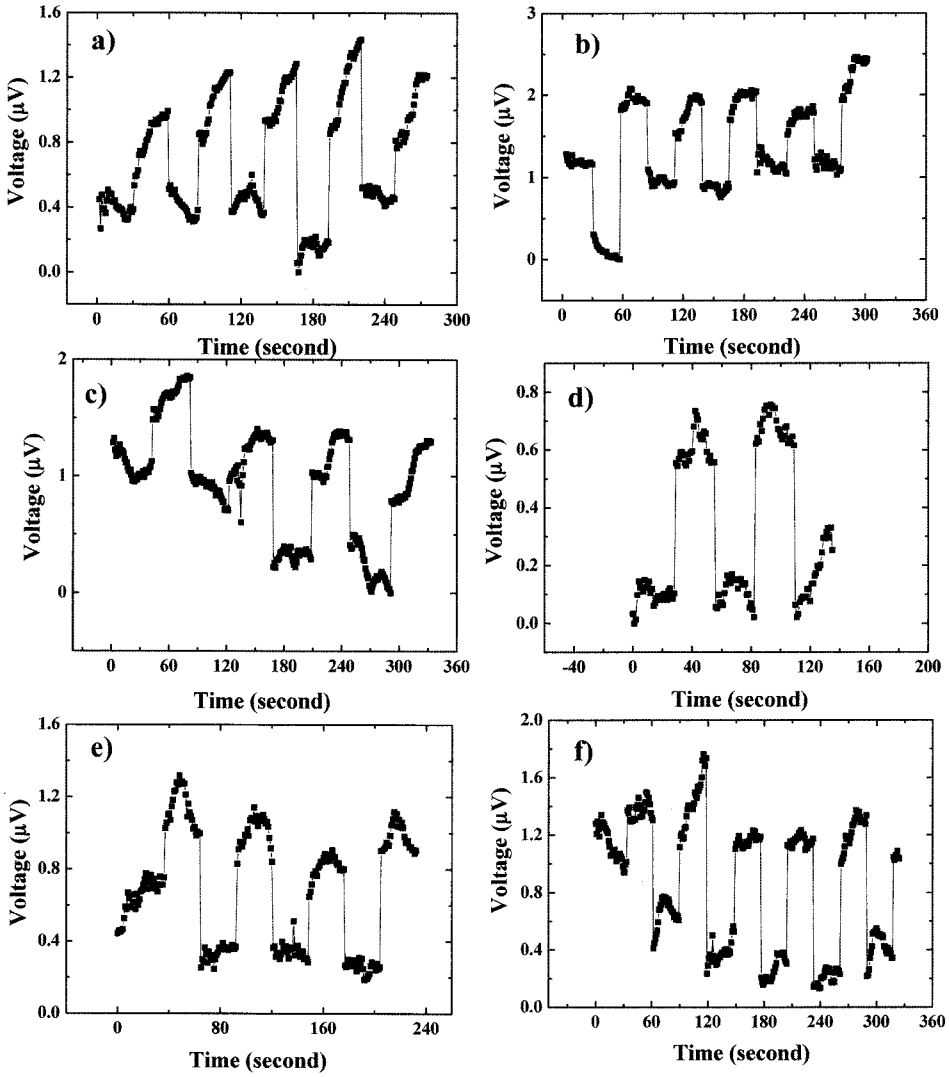

Fig. 5. Real-time sensing voltage changes at the fixed current (1 mA) for the repeated 2.8 μm magnetic beads droplet and washing by pipet-lite with volume of 2 μl per time. (a)-(f) corresponds to profiles for applied magnetic fields of H=3.0, 4.0, 5.0, 9.0, 10.0 and 11.0 Oe, respectively.

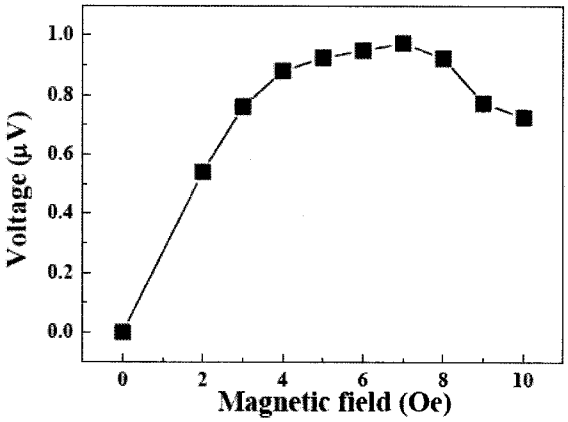

Fig. 6. The voltage change comparison of sensor signals at different applied magnetic field 0.0, 2.0, 3.0, 4.0, 5.0, 6.0, 7.0, 8.0, 9.0, 10.0 Oe and the optimum signal was obtained at 7.0 Oe.

crease from 1.0 to 0.76 μV as the magnetic field increase from 7.0 to 10.0 Oe. Therefore, the maximum signal of 1.0 μV was obtained at around 7.0 Oe.

These responses were attributed to the sensitivity of the sensor which is linear in the small external applied magnetic field regime and in the stray field induced from magnetic beads. When we increase the applied magnetic field from 0.0 to 7.0 Oe, the magnetizing field of the magnetic beads increases while the change of sensitivity is small; so that, the stray field from the magnetic beads increases as the external applied magnetic field increases, and then the output signal increases. By contrast for the applied magnetic fields from 7.0 to 10.0 Oe, the results are dominated by the change in sensitivity. At these fields, even though the magnetizing field of the magnetic bead

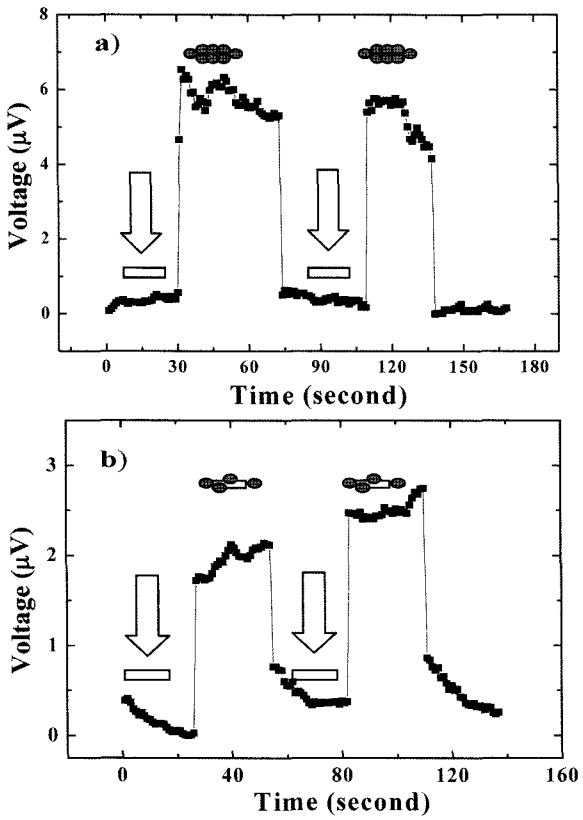

Fig. 7. Real-time voltage change for prototypal (a) and diluted (b) bead solution at magnetic field of 7.0 Oe by washing the droplet of magnetic beads by the DI water.

increases, the sensitivity of the sensor decreases much more than the change of stray field. Therefore, in total, the signal decreases in value.

Fig. 7 shows comparison of the output signals of sensor at magnetic field of 7.0 Oe for prototypal (a) and diluted (b) bead solution, in case of washing the droplet of magnetic beads by the DI water. The obtained signals were higher than those that were cleaned by pipet-lite, with output magnitude of around 6.0 μV for prototype and 3.0 μV for diluted bead solution, specially. The signals were increased because when the surface of sensor was washed cleanly by DI water, there no magnetic bead remains on the sensor. This implies when the bead solution was cleaned by pipet-lite as the first results, some magnetic beads were left at the sensor surface, as described in Fig. 7.

The bead number was counted to be around 200 beads for 50×100 μm^2 or 1 bead per 55 μm^2. This signal is quite significant for magnetic bead detection, that is, it would be possible to design a sensor for single bead detection. In fact, the output voltage is independent on the size of the Planar Hall sensor; therefore a sensor of 5×5 μm^2 or less would be capable of detecting a single magnetic bead.

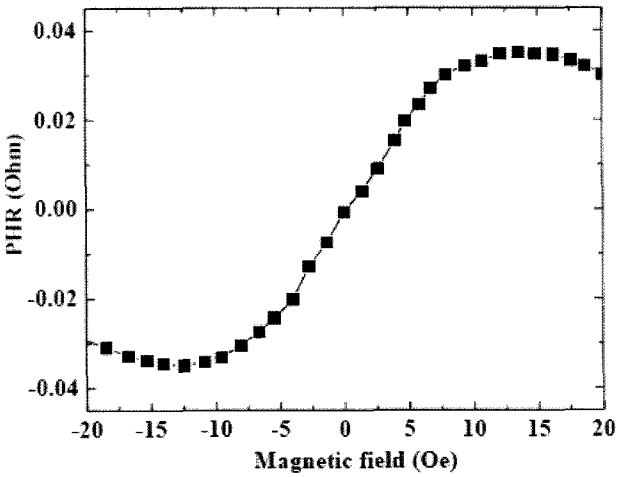

Fig. 8. The sensor transfer curve using Planar Hall effect in spin-valve structure of Ta (5.0 nm)/NiFe (6.0 nm)/Cu (3.5)/ NiFe (3.0 nm)/IrMn (10.0 nm)/Ta (5.0 nm) with the size of 33 μm^2, under various applied magnetic field at a fixed current of 1 mA.

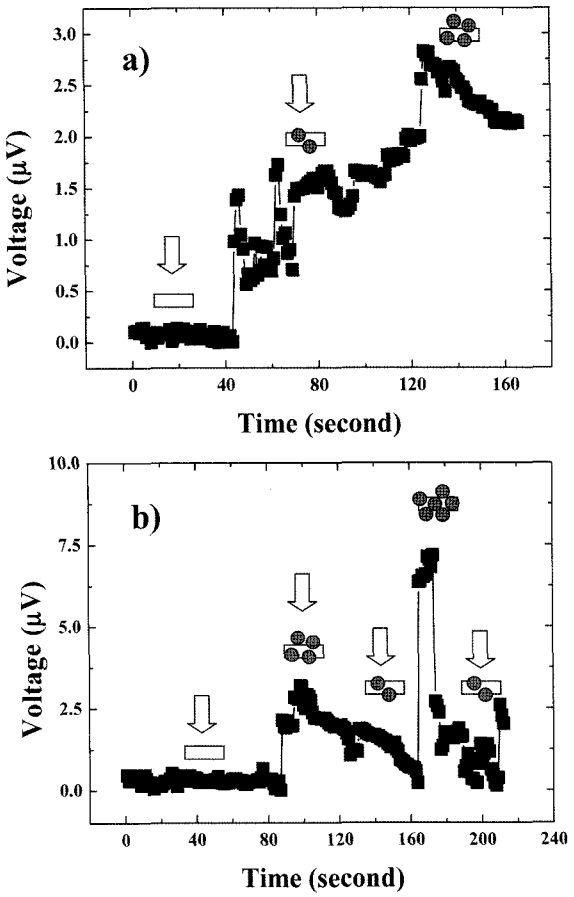

Fig. 9. Real-time profile for single Dynabeads® M-280 Streptavidin detection on 33 μm^2 Planar Hall Sensor with continuous time, at a current of 1 mA. The sensing data recorded for nonmagnetic bead, unstable position of magnetic beads (a); nonmagnetic bead, unstable position of magnetic beads and saturation signals (b).

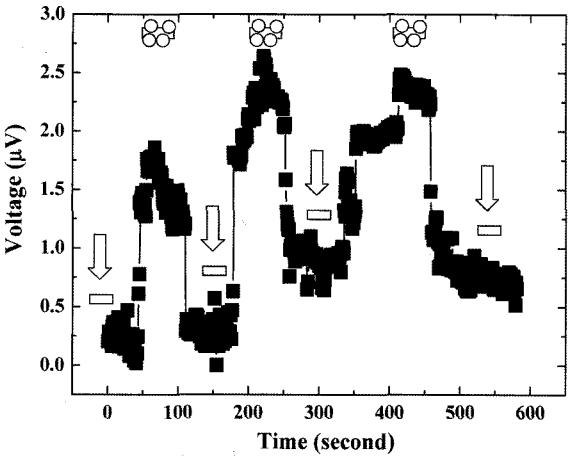

Fig. 10. Real-time profile for single Dynabeads® M-280 Streptavidin detection on 33 μm^2 Planar Hall Sensor with continuous time for three cycles of dropping and washing beads, at a current of 1.0 mA.

For the single magnetic bead detection by using sensor size of 3×3 μm^2 in the array, the single sensor transfer curve is shown in Fig. 8 where the PHR voltage is plotted versus an external applied magnetic field. From this curve, a fitting profile had been calculated by a computer fitting. Hence, a high sensitivity of linear profile would be observed around 2.5 mΩ/Oe for the bead detection.

The real-time sensing data of array were shown in Fig. 9 with the magnetic bead solution of Dynabeads® M-280 Streptavidin under a fixed current of 1.0 mA. These data were recorded at nonmagnetic bead, unstable position of magnetic beads (Fig. 9a); nonmagnetic bead, unstable position of magnetic beads and saturation signals (Fig. 9b). The unstable signals were attributed to the Brownian motion of beads in solution when they were dropped and/or washed. These motion and vibration would be reduced if it was measured for several ten seconds waiting after dropping and before washing magnetic bead solution. The changes between dropped and washed bead solution are rapidly and the magnitude of signal is around 1.4 μV.

4. Conclusions

The spin-valve structure of Ta (5.0 nm)/NiFe (4.5 nm)/CoFe (1.5 nm)/Cu (2.6 nm)/CoFe (4.0 nm)/IrMn (10.0 nm)/Ta (5.0 nm) was applied and demonstrated to detect the Dynabeads® M-280 as a biosensor including a high sensitivity and small number of single magnetic beads. The results of real-time profiles revealed stable and significant signals at external applied magnetic field of around 7.0 Oe with the resolution of 0.04 beads per μm^2 when the face of sensor was washed by DI water. Consequently, a successful array including 24 patterns with the single sensor size of 3×3 μm^2 has shown the uniform and stable signals for single magnetic bead detection. The comparison of this sensor signal with the others has proved feasibility for biosensor application. This, connecting with the advantages of more stable and high signal to noise of PHR sensor's behaviors, can be used for the biomolcular recognition and provide a vehicle for detection and study of other molecular interaction.

References

[1] M. M. Miller, P. E. Edelstein, C. R. Tamanaha, L. Zhong, S. Bounak, L. J. Whitman, and R. J. Colton, J. Magn. Magn. Mater. **225**, 138 (2001).
[2] D. L. Graham, H. Ferreira, J. Bernado, P. P. Freitas, and J. M. S. Cabral, J. Appl. Phys. **91**, 7786 (2002).
[3] D. L. Graham, H. A. Ferreira, P. P. Freitas, and J. M. S. Cabral, Biosens. Bioelectron. **18**, 483 (2003).
[4] P. Besse, G. Boero, M. Demierre, V. Pott, and R. Popovic, Appl. Phys. Lett. **80**, 4199 (2002).
[5] A. Sandhu, H.Sanbonsugi, I. Shibasaki, M. Abe, and H. Handa, Jpn. J. Appl. Phys. **43**, L868 (2004).
[6] L. Ejsing, M. F. Hansen, A. K. Menon, H. A. Ferreira, D. L. Graham, and P. P. Fretas, Appl. Phys. Lett. **84**, 4729 (2004).
[7] A. Schuhl, F. Nguyen Van Dau, and J. R. Childress, Appl. Phys. Lett. **66**, 2751 (1995).
[8] F. Nguyen Van Dau, A. Schuhl, J. R. Childress, and M. Sussiau, Sensors and Actuators A **53**, 256 (1996).
[9] M. Johnson, Magnetoelectronics, Elsevier, Amsterdam, 2004.
[10] L. Ejsing, M. F. Hansen, A. K. Menon, H. A. Ferreira, D. L. Graham, and P. P. Freitas, J. Magn. Magn. Mater. **293**, 677 (2005).
[11] N. T. Thanh, M. G. Chun, N. D. Ha, K. Y. Kim, C. O. Kim, and C. G. Kim, J. Magn. Magn. Mater. **304**, e84 (2006).